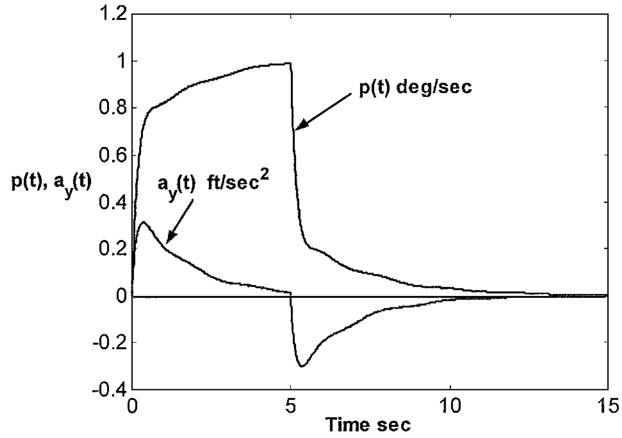

Fig. 2 Response of aircraft to unit pulse roll-rate p command.

the use of Eq. (20a) would not be justified here because one could not assume that a_y is tightly constrained.

This exercise suggests a sequential loop-closure design procedure with the p and a_y variables paired with δ_a and δ_r, respectively, closing the p loop first. Had matrix $K(s)$ in Fig. 1 not been the identity matrix, an analysis similar to that just completed could be undertaken with the transfer functions of Eq. (19) obtained from $P'(s) = P(s)K(s)$ and those of Eq. (20) obtained from relationships such as Eq. (14). In cases in which there are no NMP transmission zeros, pairing input–output variables and selecting loop-closure sequences could be based on the required compensation in each loop. The form of this compensation could be estimated from equations similar to Eqs. (19) and (20).

Figure 1 can serve as a diagram for the SCAS, now with $y_1(s) = p(s)$, $y_2(s) = a_y(s)$, $u_1(s) = \delta_a(s)$, $u_2(s) = \delta_r(s)$, and $K(s) = I$. The compensator $G_1(s)$ in Fig. 1 was obtained using standard loop-shaping techniques.[8] The result was a 5 rad/s open-loop crossover frequency with

$$G_1(s) = \frac{0.074(3)(0.1)^2}{(0)^2(0.2)} \tag{21}$$

The effective plant for the second loop closure [now determined using the actual $G_1(s)$ of Eq. (21)] is given by

$$\left.\frac{a_y}{\delta_r}\right|_{p\to\delta_a} = \frac{0.6075(15.71)(4.833)(-6.11)(1.147)}{[0.962, 3.385][0.131, 2.943]} \tag{22}$$

Because of the NMP zero in the numerator at $s = 6.11$, the maximum practical crossover frequency for this loop with acceptable stability margins is approximately 1 rad/s. Again, a compensator was obtained using standard loop-shaping techniques and is given by

$$G_2(s) = \frac{-1.42[0.15, 3]}{(0)(50)} \tag{23}$$

The response of the aircraft to a 5-s unit pulse command in p with this SCAS is shown in Fig. 2. Similar command following and off-axis responses result when a unit pulse command in a_y is employed.

Conclusions

The use of coupling numerators based on output equations as opposed to state equations results in a simplification of the coupling numerator expressions. The use of these simplified numerators in square control systems with response variables assumed to be tightly constrained provides insight into the selection of appropriate pairings of plant inputs and outputs for square feedback designs. In addition, it demonstrates the effect of transmission zeros on individual effective plant transfer function elements, when other response variables are tightly constrained.

References

[1]McRuer, D., Ashkenas, I., and Graham, D., *Aircraft Dynamics and Automatic Control*, Princeton Univ. Press, Princeton, NJ, 1973, Chap. 3.

[2]Heffley, R. K., "A Compilation and Analysis of Helicopter Handling Qualities Data," NASA CR-3144, March 1979.

[3]Catapang, D. R., Tischler, M. B., and Biezad, D. J., "Robust Crossfeed Design for Hovering Rotorcraft," *International Journal of Control*, Vol. 4, No. 1, 1994, pp. 161–180.

[4]Stengel, R. F., *Stochastic Optimal Control*, Wiley, New York, 1986, p. 544.

[5]Horowitz, I., *Quantitative Feedback Theory*, QFT Publications, Boulder, CO, 1993.

[6]Wells, S. R., and Hess, R. A., "MIMO Sliding Mode Control for a Tailless Fighter Aircraft," *Journal of Guidance, Control, and Dynamics* (to be published).

[7]Rivard, G. R., "Weighting Matrix Selection for QFT Designs," M.S. Thesis, Air Force Inst. of Technology, No. AFIT/GE/ENG/89D-43, Wright–Patterson AFB, OH, Dec. 1989.

[8]Maciejowski, J. M., *Multivariable Feedback Design*, Addison–Wesley, Wokingham, England, U.K., 1989, Chap. 1.

Inverse Solar Sail Trajectory Problem

Colin R. McInnes*
University of Glasgow,
Glasgow, Scotland G12 8QQ, United Kingdom

I. Introduction

SOLAR sailing has long been considered for a diverse range of future mission applications. Although low-performance solar sails can be utilized for interplanetary transfer using heliocentric spiral trajectories, high-performance solar sails can enable exotic applications using non-Keplerian orbits. A simple example of such an exotic application is "levitation," with the solar radiation pressure acceleration experienced by the sail exactly balancing solar gravity. Such a static equilibrium allows the solar sail to remain stationary with respect to the sun, or indeed if the sail is turned edgewise to the sun it will fall sunwards on a rectilinear trajectory. Although this static equilibrium is simple to identify, the question of transfer to it from an Earth escape trajectory remains open. This Note will derive an analytic sail steering law that allows the solar sail is be maneuvered from a circular heliocentric orbit, to a static equilibrium location at the same heliocentric distance. The required trajectory will be defined a priori with the resulting sail steering law derived from the equations of motion. An inverse trajectory problem is, therefore, being solved.

II. Static Equilibria

To identify conditions for static equilibria, the equations of motion for the solar sail will now be defined. The heliocentric equations of motion for an ideal, planar solar sail may be written in plane polar coordinates (r, θ) as[1]

$$\ddot{r} - r\dot{\theta}^2 = -(\mu/r^2)(1 - \beta\cos^3\alpha) \tag{1a}$$

$$r\ddot{\theta} + 2\dot{r}\dot{\theta} = \beta(\mu/r^2)\cos^2\alpha\sin\alpha \tag{1b}$$

where r is the heliocentric distance of the solar sail from the sun and θ is the polar angle of the solar sail, measured anticlockwise from some reference position. Because both solar radiation pressure and solar gravity have an inverse square variation, the solar sail performance can be parameterized by the sail lightness number β,

---

Received 12 February 2002; revision received 12 June 2002; accepted for publication 17 September 2002. Copyright © 2002 by Colin R. McInnes. Published by the American Institute of Aeronautics and Astronautics, Inc., with permission. Copies of this paper may be made for personal or internal use, on condition that the copier pay the $10.00 per-copy fee to the Copyright Clearance Center, Inc., 222 Rosewood Drive, Danvers, MA 01923; include the code 0731-5090/03 $10.00 in correspondence with the CCC.

*Professor, Department of Aerospace Engineering; colinmc@aero.gla.ac.uk.

defined as the ratio of the solar radiation force to solar gravitational force acting on the solar sail. The sail pitch angle α is defined as the angle between the sun-sail line and the sail normal.

It can be seen from Eq. (1) that an equilibrium solution is available if $\alpha = 0$ and $\beta = 1$ with the solar sail stationary at a fixed heliocentric distance. Because both solar radiation pressure and solar gravity have an inverse square variation, such an equilibrium is possible at any heliocentric distance. It can be shown that the equilibrium has marginal stability, with perturbations growing as a linear function of time.[1] This becomes clear by noting that the solar sail has no net force acting on it if it is displaced because both solar radiation pressure and solar gravity have an inverse square variation.

III. Transfer to Static Equilibria

A sail steering law will now be sought that transfers the solar sail from a circular Keplerian orbit at some heliocentric distance $\tilde{r}$, to a static equilibrium at the same heliocentric distance. The constraint that $\dot{r} = \ddot{r} = 0$ will, therefore, be imposed on Eq. (1), leading to a reduced set of equations of motion defined by

$$\dot{\theta}^2 = \omega^2(1 - \cos^3\alpha) \tag{2a}$$

$$\ddot{\theta} = \omega^2\cos^2\alpha\sin\alpha \tag{2b}$$

where $\omega = \sqrt{(\mu/\tilde{r}^3)}$. It can be seen that Eq. (2a) defines the sail pitch angle α as a function of the orbital angular velocity $\dot{\theta}$ so that

$$\cos\alpha = [1 - (\dot{\theta}/\omega)^2]^{\frac{1}{3}} \tag{3}$$

Therefore, if $\dot{\theta} = \omega$, the required sail pitch angle $\alpha = -\pi/2$, and if $\dot{\theta} = 0$, then required sail pitch angle $\alpha = 0$, corresponding to the conditions for a circular Keplerian orbit and static equilibrium, respectively. These two states represent the boundary conditions for the transfer problem at hand. When Eq. (2a) is differentiated, it can now be shown that

$$\ddot{\theta} = \frac{3}{2}\omega\frac{\cos^2\alpha\sin\alpha}{\sqrt{1 - \cos\alpha^3}}\dot{\alpha} \tag{4}$$

However, when Eq. (4) and Eq. (2b) are equated, it can be seen that

$$\dot{\alpha} = \tfrac{2}{3}\omega\sqrt{1 - \cos^3\alpha} \tag{5}$$

which provides an auxiliary equation to add to Eq. (1) with boundary condition $\alpha(0) = -\pi/2$. Integrating Eq. (5) provides the sail steering law to ensure that $\dot{r} = \ddot{r} = 0$ while $\dot{\theta} \rightarrow 0$ as $\alpha \rightarrow 0$. In addition, Eq. (5) can be used to provide the transfer duration T as

$$T = \frac{3}{2\omega}\int_{-\pi/2}^{0}\frac{\mathrm{d}\alpha}{\sqrt{1 - \cos^3\alpha}} \tag{6}$$

It can be seen from Eq. (6) that the integral does not converge as $\alpha \rightarrow 0$, indicating that the transfer duration is infinite. In fact, approach to the static equilibrium is indeed asymptotic, but the practical duration of the transfer is of order 550 days, as will be discussed. The effective Δv for the transfer is of order $\sqrt{(\mu/\tilde{r})}$.

A more compact form for the sail steering law can be obtained by noting that Eq. (5) may be rewritten using Eq. (2a) as

$$\frac{\mathrm{d}\theta}{\mathrm{d}\alpha} = \frac{3}{2} \tag{7}$$

which can be immediately integrated with the appropriate boundary condition to give

$$\alpha(\theta) = \tfrac{2}{3}\theta - (\pi/2) \tag{8}$$

Because the solar sail approaches static equilibrium as $\alpha \rightarrow 0$, the transfer angle for the maneuver can be obtained from Eq. (8) as $3\pi/4$, which is independent of the heliocentric distance $\tilde{r}$. In addition, it is clear that $\dot{\alpha} = 2\dot{\theta}/3$. so that the turn rate of the sail is proportional to the instantaneous orbital angular velocity. Such a simple steering law is likely to be advantageous to implement in practice.

IV. Application

To demonstrate the sail steering law that has been derived, a solar sail with a lightness number $\beta = 1$ will be considered moving along a circular Keplerian orbit at 1 astronomical unit (AU). This is representative of a solar sail deployed on a parabolic Earth escape trajectory. The steering law defined by Eq. (5) [or Eq. (8)] is then used to transfer the solar sail to a static equilibrium at 1 AU. The resulting trajectory obtained by integrating the system of equations obtained from Eq. (1) and Eq. (5) is shown in Fig. 1. As expected, the sail steering law enforces the constraint $\dot{r} = \ddot{r} = 0$. The resulting sail pitch time history is shown in Fig. 2, with an asymptotic approach to the static equilibrium as $\alpha \rightarrow 0$. Furthermore, the sail polar angle and orbital angular velocity are shown in Figs. 3 and 4, where it can be seen that the effective transfer duration is of order 550 days, with a transfer angle of exactly $3\pi/4$.

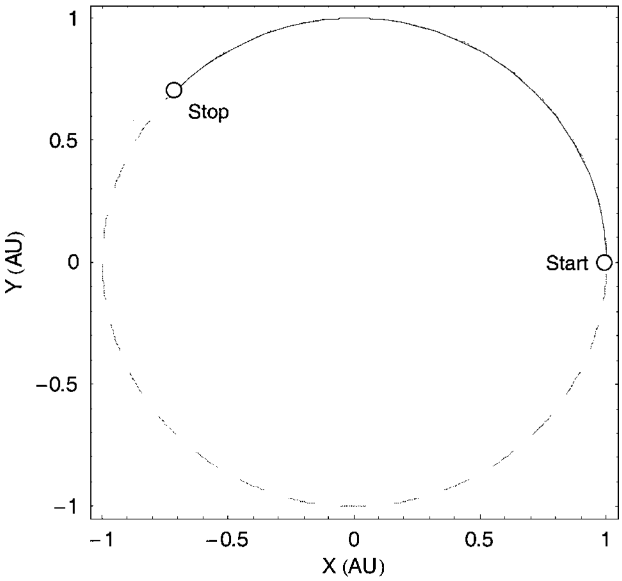

Fig. 1 Transfer to static equilibrium: ○, start, stop.

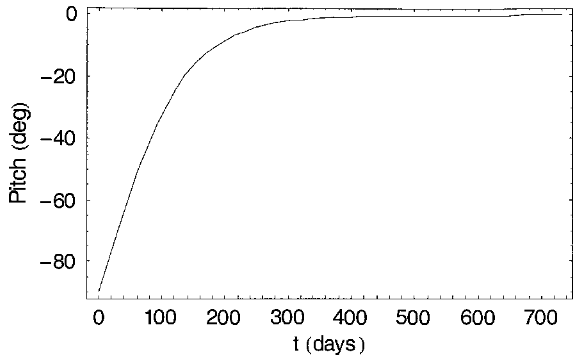

Fig. 2 Solar sail pitch angle time history.

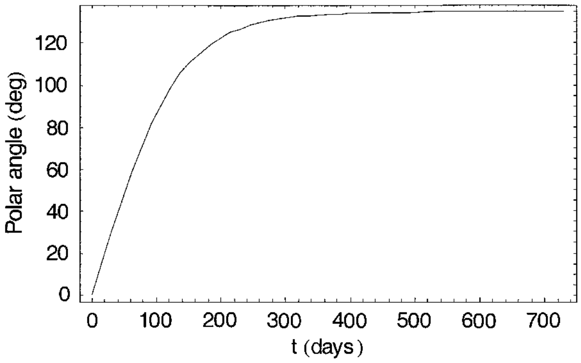

Fig. 3 Solar sail polar angle time history.

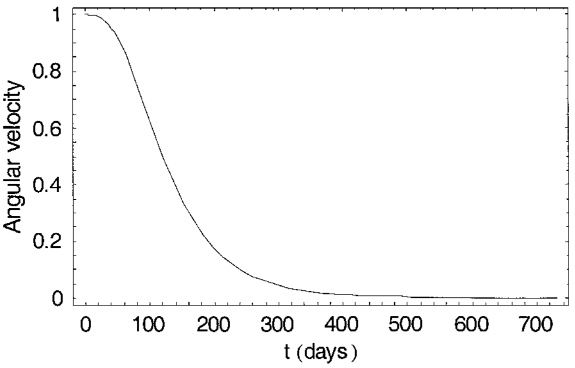

Fig. 4 Orbital angular velocity time history (normalized to initial orbital angular velocity).

V. Conclusions

A sail steering law has been derived in closed-form which transfers a solar sail with a lightness number $\beta = 1$ from a circular heliocentric orbit to a static equilibrium at the same heliocentric distance. The steering law is obtained as the solution to a first order ordinary differential equation, or is parameterized with respect to the solar sail polar angle. Independent of the starting orbit, it has been shown that the transfer angle for the maneuver is always $3\pi/4$.

Acknowledgment

This work was supported by the Leverhulme Trust.

Reference

[1]McInnes, C. R., *Solar Sailing: Technology, Dynamics and Mission Applications*, Springer-Verlag, London, 1999, pp. 118, 119.

Composite Estimate of Spacecraft Sensor Alignment Calibrations

Mark E. Pittelkau[*]
Johns Hopkins University, Applied Physics Laboratory,
Laurel, Maryland 20723-6099

Introduction

Alignment Kalman filters (AKFs) for spacecraft sensor alignment calibration were developed in Refs. 1 and 2. There it was shown how to model attitude sensor misalignment and gyro calibration parameters and how to implement these models in a Kalman filter using the upper triangular diagonal (UD) factorization method of Bierman.[3] The efficacy of the calibration estimators in Refs. 1 and 2 was shown in simulation results using an attitude maneuver that makes all of the parameters observable.

Sensor alignment and calibration is of importance to the spacecraft community because the time and effort required for calibration is not trivial, calibration maneuvers could interfere with mission operation, and inadequate calibration can result in poor attitude knowledge and poor pointing performance. A problem in attitude sensor and gyro calibration is that a single attitude maneuver profile may not be sufficient to estimate all of the calibration parameters with small covariance because observability of the gyro parameters depends on the maneuver. Restrictions on such a maneuver may be due to physical, operational, or design constraints. The use of only one maneuver profile might also not be desirable because small thermal effects on alignment and gyro parameters could bias the calibration estimates. The constraints on the system considered in this Note are that no special calibration maneuvers be required and that calibration be performed using only normal Earth scanning maneuvers. Thermal distortion is the one of the drivers for the latter.

The objective of this Note is to introduce the technique of combining several estimated calibration parameter sets to obtain a composite least-squares estimate that has smaller covariance than all of the individual estimates. An algorithm is developed to compute the composite estimate from the estimated calibration parameter sets and the UD-factored covariances produced by the AKF. The algorithm utilizes the UD factors directly in a recursive, computationally efficient, and numerically reliable manner. It will be shown via simulation results that, with an appropriate set of attitude maneuvers, all parameters can be estimated with small covariance, even if some parameters (or linear combination of parameters) are of limited accuracy due to maneuver restrictions.

This idea of a composite estimator is not unlike the two-stage estimator in Ref. 4, where the final estimates from several executions of a first-stage estimator are used as measurements in a second-stage estimator.

A mathematical statement of the problem is given in the next section followed by the Kalman filter solution. Simulation results show the effectiveness of combining calibration parameter estimates that result from various maneuver scenarios. Results are shown for idealized maneuvers and for a set of realistic maneuvers for an Earth-imaging spacecraft.

Preliminaries

The AKFs reported in Refs. 1 and 2 produce a set of attitude, gyro bias, and calibration parameter estimates and the UD factors of the covariance matrix by processing attitude sensor data collected during a calibration maneuver. Let $\hat{\mathbf{x}}$ be the vector of estimated calibration parameters at the end of the calibration maneuver and let R be its covariance. The UD factors of R can be obtained directly from the UD factors of the covariance matrix $\boldsymbol{P}$ from the Kalman filter. There are $m = 6$ attitude perturbation and gyro bias states and n calibration parameters in the filter state vector. Partitioning $\boldsymbol{P}$ and its UD factors gives

$$
\begin{aligned}
\boldsymbol{P} &= \begin{array}{c} \begin{array}{cc} \overbrace{\qquad}^{m} & \overbrace{\qquad}^{n} \end{array} \\ \begin{bmatrix} \boldsymbol{P}_{11} & \boldsymbol{P}_{12} \\ \boldsymbol{P}_{21} & \boldsymbol{P}_{22} \end{bmatrix} \begin{array}{l} \}m \\ \}n \end{array} \end{array} \\
&= \boldsymbol{U}\boldsymbol{D}\boldsymbol{U}^{T} \\
&= \begin{bmatrix} U_{11} & U_{12} \\ 0 & U_{22} \end{bmatrix} \begin{bmatrix} D_{1} & 0 \\ 0 & D_{2} \end{bmatrix} \begin{bmatrix} U_{11}^{T} & 0 \\ U_{12}^{T} & U_{22}^{T} \end{bmatrix} \\
&= \begin{bmatrix} U_{11}D_{1}U_{11}^{T} + U_{12}D_{2}U_{12}^{T} & U_{12}D_{2}U_{22}^{T} \\ U_{22}D_{2}U_{12}^{T} & U_{22}D_{2}U_{22}^{T} \end{bmatrix}
\end{aligned}
\tag{1}
$$

where $\boldsymbol{U}$ is unit upper triangular and $\boldsymbol{D}$ is diagonal. Thus $\boldsymbol{P}_{22} = U_{22}D_{2}U_{22}^{T} \overset{\Delta}{=} R$, so that the UD factors of the parameter error covariance R are simply the partitions U_{22} and D_{2} of the UD factorization of $\boldsymbol{P}$. If the UD factorization of $\boldsymbol{P}$ is stored in packed form, then the packed form of U_{22} and D_{2} is extracted by skipping the first $m(m+1)/2 + mn$ elements of the packed UD factors of $\boldsymbol{P}$. To simplify notation in the developments that follow, let $U = U_{22}$ and $D = D_{2}$ so that $R = UDU^{T}$.

The AKF is run N times to process attitude and gyro data from each of N separate calibration maneuvers. Thus, we have N estimated calibration parameter vectors $\hat{\mathbf{x}}_{1}, \hat{\mathbf{x}}_{2}, \ldots, \hat{\mathbf{x}}_{N}$ and UD factors of the covariance matrices $R_{1}, R_{2}, \ldots, R_{N}$, each $\hat{\mathbf{x}}_{k}$ and R_{k} being the final value at the end of the AKF run. These estimates can be regarded as noisy observations $\boldsymbol{y}_{1}, \boldsymbol{y}_{2}, \ldots, \boldsymbol{y}_{N}$ of the true parameter

---

Received 4 December 2001; revision received 11 September 2002; accepted for publication 10 October 2002. Copyright © 2002 by the American Institute of Aeronautics and Astronautics, Inc. All rights reserved. Copies of this paper may be made for personal or internal use, on condition that the copier pay the $10.00 per-copy fee to the Copyright Clearance Center, Inc., 222 Rosewood Drive, Danvers, MA 01923; include the code 0731-5090/03 $10.00 in correspondence with the CCC.

[*] Senior Professional Staff, Space Department; mittelkau@ieee.org. Senior Member AIAA.